Appendix B: Supplemental Information

Method for adding disorder in network connectivity.

In the main text, the method to build networks resulted in a connectivity (adjacency matrix A_{ij}) of that of a triangular lattice. To introduce disorder in the connectivity we place nodes on a triangular lattice with their positions given by $\mathbf{R}_i^{\rm lat}$. The nodes are then displaced by a random uniform perturbation $\Delta\mathbf{R}_i \sim ([-\epsilon,\epsilon],[-\epsilon,\epsilon])$ to achieve a disordered structure $\mathbf{R}_i^{\rm dis} = \mathbf{R}_i^{\rm lat} + \Delta\mathbf{R}_i$. An adjacency matrix is defined as follows,

$$A_{ij} = \begin{cases} 1, & i \neq j \text{ and } ||\mathbf{R}_{\rm i}^{\rm dis} - \mathbf{R}_{\rm j}^{\rm dis}|| < {\rm c} \\ 0, & \text{otherwise} \end{cases}$$

The value of c is chosen such that the mean coordination $z = \sum_{ij} A_{ij}/N$ takes a desired value.

3d Networks

Three dimensional networks share the same definition as 2d networks (Eq. (A1), (A2), (A3)) except for the following differences: $\mathbf{r}_i = (x_i, y_i, z_i)$, nodes are initially placed on a 3d hexagonal closed packed lattice rather than 2d triangular lattice, and $\Delta\mathbf{R}_i \sim ([-a\epsilon, a\epsilon],[-a\epsilon, a\epsilon],[-a\epsilon, a\epsilon])$. The values of the distance cutoff and spring constant for the harmonic repulsion term remain the same in 3d, $\ell_{\rm rep} = 0.7$ and $k_{\rm rep} = 2$.

1d model at zero temperature

For a system of harmonic springs, the energy takes the form,

$$V(x) = \frac{1}{2}\sum_i k_i(x-\ell_i)^2 = \frac{1}{2}\left(\sum_i k_i\right)\left(x - \frac{\sum_i k_i\ell_i}{\sum_i k_i}\right)^2 + V_{\rm min} \tag{B1}$$

where

$$V_{\rm min} = \min_x V(x) = \frac{1}{2}\left(\sum_i k_i\ell_i^2 - \frac{(\sum_i k_i\ell_i)^2}{\sum_i k_i}\right). \tag{B2}$$

The 1d model of allostery is given by

$$U(x) = \frac{1}{2}k_a(x-\ell_{\rm act})^2 + \frac{1}{2}k_a(x-\ell_{\rm allo})^2 + \frac{1}{2}k_m(|x|-\ell_m)^2. \tag{B3}$$

Putting (B3) in the form of (B1) gives

$$V(x,\ell_m) = \frac{1}{2}(2k_a+k_m)\left(x - \frac{k_a(\ell_{\rm act}+\ell_{\rm allo}) + k_m\ell_m}{2k_a+k_m}\right)^2 + V_{\rm min}(\ell_m) \tag{B4}$$

where

$$V_{\rm min}(\ell_m) = \frac{1}{2}\left[k_a(\ell_{\rm act}^2+\ell_{\rm allo}^2) + k_m\ell_m^2 - \frac{(k_a(\ell_{\rm act}+\ell_{\rm allo}) + k_m\ell_m)^2}{2k_a+k_m}\right]. \tag{B5}$$

$U(x)$ can be written as the piecewise function,

$$U(x) = \begin{cases} V(x,-\ell_m), & x \leq 0 \\ V(x,\ell_m), & x > 0. \end{cases} \tag{B6}$$

The ground state of U is defined by $E = \min_x U(x) = \min_\pm V_{\rm min}(\pm\ell_m)$. Taking the physical conditions $k_a > 0$, $k_m > m$ and $\ell_m > 0$, this gives

$$E(\ell_{\rm act},\ell_{\rm allo}) = \frac{k_a}{2(2k_a+k_m)}\left(k_a(\ell_{\rm act}-\ell_{\rm allo})^2 + k_m(\ell_{\rm act}^2+\ell_{\rm allo}^2+2\ell_m^2) - 2k_m|(\ell_{\rm act}+\ell_{\rm allo})\ell_m|\right) \tag{B7}$$

Cooperative allostery is computed as

$$\Delta\Delta E = E(\ell_1, \ell_0) + E(\ell_0, \ell_1) - E(\ell_1, \ell_1) - E(\ell_0, \ell_0), \tag{B8}$$

where ℓ_0 and ℓ_1 represent the solvent and the ligand, respectively. In the 1d model $\Delta\Delta E$ reduces to,

$$\Delta\Delta E = \frac{k_a}{2k_a + k_m}\left(k_a|\ell_1 - \ell_0|^2 + 2k_m|\ell_m|(|\ell_1| + |\ell_0| - |\ell_1 + \ell_0|)\right). \tag{B9}$$

If $\ell_1 = -\ell_0$ and $\delta = |\ell_1 - \ell_0|$,

$$\Delta\Delta E = \frac{k_a(k_a\delta + 2k_m\ell_m)\delta}{2k_a + k_m}. \tag{B10}$$

The mechanism changes from single-state to multi-state at the transition rest length $\ell_m^* = \delta/4$. When $\ell_m < \delta/4$, $\Delta\Delta E$ is optimized at $k_m = 0$ and can not exceed $k_a\delta^2/2$. When $\ell_m > \delta/4$, $\Delta\Delta E$ is optimized at $k_m = \infty$ and can take arbitrarily large values ($\Delta\Delta E = 2k_a\ell_m\delta$). The first term in (B10) is the contribution from being able to actuate the (potentially) soft allosteric mode and the second term is the contribution from the two-state switch.

1d model at finite temperature

In the canonical ensemble, the partition function Z of a system with energy $U(x) = kx^2/2$ at temperature T (the Boltzmann constant is folded in T such that T has units of energy) is given by

$$Z = \int e^{-E(x)/T}dx = \int_{-\infty}^{\infty} e^{-kx^2/2T}dx = \sqrt{\frac{2\pi T}{k}}, \tag{B11}$$

and its free energy is

$$F = -T\ln Z = \frac{T}{2}\ln\frac{k}{2\pi T}. \tag{B12}$$

The energy of the 1d model (B3) takes the form of two parabolas that abut at $x = 0$. The partition function is

$$Z = \int_{-\infty}^{0} e^{-V(x,-\ell_m)/T}dx + \int_{0}^{\infty} e^{-V(x,\ell_m)/T}dx \tag{B13}$$

Setting $\kappa = 2k_a + k_m$ and $\lambda(\ell_m) = (k_a(\ell_{\rm act} + \ell_{\rm allo}) + k_m\ell_m)/(2k_a + k_m)$ gives

$$Z = e^{-V_{\min}(-\ell_m)/T}\int_{-\infty}^{0} e^{-\kappa(x-\lambda(-\ell_m))^2/2T}dx + e^{-V_{\min}(\ell_m)/T}\int_{0}^{\infty} e^{-\kappa(x-\lambda(\ell_m))^2/2T}dx \tag{B14}$$

$$= \frac{1}{2}\sqrt{\frac{\pi T}{\kappa}}\left[e^{-V_{\min}(-\ell_m)/T}\left(1 + \mathrm{erf}\left(-\sqrt{\frac{\kappa}{2\mathrm{T}}}\lambda(-\ell_{\rm m})\right)\right) + e^{-V_{\min}(\ell_m)/T}\left(1 + \mathrm{erf}\left(\sqrt{\frac{\kappa}{2\mathrm{T}}}\lambda(\ell_{\rm m})\right)\right)\right] \tag{B15}$$

where erf is the error function.

In the limit where $k_m/k_a \to \infty$ the energy simplifies to

$$U(x) = \begin{cases} \frac{k_a}{2}\left((x-\ell_{\rm act})^2 + (\ell_m - \ell_{\rm allo})^2\right) & x = -\ell_m \\ \frac{k_a}{2}\left((x-\ell_{\rm act})^2 + (\ell_m - \ell_{\rm allo})^2\right) & x = \ell_m \\ \infty & \text{otherwise} \end{cases} \tag{B16}$$

and the free energy becomes

$$F(\ell_{\rm act}, \ell_{\rm allo}) = -T\ln\left[e^{-\frac{k_a}{2T}((\ell_m+\ell_{\rm act})^2+(\ell_m+\ell_{\rm allo})^2)} + e^{-\frac{k_a}{2T}((\ell_m-\ell_{\rm act})^2+(\ell_m-\ell_{\rm allo})^2)}\right] \tag{B17}$$

Taking $\ell_0 = -\delta/2$ and $\ell_1 = \delta/2$ the cooperativity is

$$\Delta\Delta F = F(\delta/2, -\delta/2) + F(-\delta/2, \delta/2) - F(\delta/2, \delta/2) - F(-\delta/2, -\delta/2), \tag{B18}$$

and after some algebra,

$$\Delta\Delta F = 2T \ln\cosh\left(k_a \ell_m \delta / T\right). \tag{B19}$$

In the opposite limit where $k_m/k_a \to 0$,

$$U(x) = \frac{k_a}{2}(x-\ell_{\rm act})^2 + \frac{k_a}{2}(x-\ell_{\rm allo})^2 \tag{B20}$$

$$= k_a\left(x - \frac{\ell_{\rm act}+\ell_{\rm allo}}{2}\right)^2 + \frac{k_a}{4}\left(\ell_{\rm act}-\ell_{\rm allo}\right)^2 \tag{B21}$$

$$\tag{B22}$$

and the free energy is

$$F(\ell_{\rm act},\ell_{\rm allo}) = \frac{k_a}{4}(\ell_{\rm act}-\ell_{\rm allo})^2 - \frac{T}{2}\ln\frac{\pi T}{k_a} \tag{B23}$$

Taking $\ell_0 = -\delta/2$ and $\ell_0 = \delta/2$ the cooperativity is

$$\Delta\Delta F = F(\delta/2,-\delta/2) + F(-\delta/2,\delta/2) - F(\delta/2,\delta/2) - F(-\delta/2,-\delta/2) \tag{B24}$$

and after some algebra

$$\Delta\Delta F = \frac{1}{2}k_a\delta^2. \tag{B25}$$

When $T > 0$ the transition point between mechanisms occurs for

$$\ell_m^*(T) = \frac{T}{k_a\delta}\ln\left[e^{k_a\delta^2/4T} + \sqrt{e^{k_a\delta^2/2T}-1}\right] \tag{B26}$$

Thermodynamical models

Our models can be coarse-grained to obtain a thermodynamical description comparable to the formulation of the MWC and KNF models. This is achieved by defining "states" with given free energies, from which equilibrium probabilities are computed from Boltzmann's law. A state corresponds in our models to a distinct local minimum of the energy or free energy landscape. At finite temperatures, a further requirement is that the free energy barriers are large relative to the temperature so that a local equilibrium occurs within the states. If two states have free energies F_1 and F_2 with a maximum $F^\dagger$ along the conformational coordinate that connects them, this assumption amounts to $F^\dagger - \max(F_1,F_2) \ll T$ in units where the Boltzmann constant is $k_B = 1$. A description can also be given in terms of kinetic rates $k_{1\to2}$ and $k_{2\to1}$ for the transition between the states, which may, for instance, be of the form $k_{1\to2} = k_0 e^{-(F^\dagger - F_1)/T}$ and $k_{2\to1} = k_0 e^{-(F^\dagger - F_2)/T}$.

One possible coarse-graining of the 1d model could assert that two conformational states exist: state T corresponding to $x < 0$ and state R corresponding to $x > 0$. This coarse-graining separates the two states by the barrier at $x = 0$. With two binding sites, there would be a total of eight states: T00, T10, T01, T11, R00, R10, R01, R11 (the last two digits represent the state of ligand binding as in Figure 1). Taking ℓ_0 and ℓ_1 to be the rest lengths of the springs representing the unbound and bound states, the free energies of the eight states are,

$$F_{Tij} = -T\ln\left(\int_{-\infty}^{0} e^{-\frac{1}{2}\left(k_a(x-\ell_i)^2 + k_a(x-\ell_j)^2 + k_m(x+\ell_m)^2\right)/T}dx\right) \tag{B27}$$

$$F_{Rij} = -T\ln\left(\int_{0}^{\infty} e^{-\frac{1}{2}\left(k_a(x-\ell_i)^2 + k_a(x-\ell_j)^2 + k_m(x-\ell_m)^2\right)/T}dx\right) \tag{B28}$$

A quantity of particular interest is the fraction of occupied binding sites Y at a ligand concentration c,

$$Y(c) = 0 * P_{00}(c) + \frac{1}{2} * P_{01}(c) + \frac{1}{2} * P_{10}(c) + 1 * P_{11}(c) \tag{B29}$$

$$Y(c) = \frac{ce^{-F_{T10}/T} + ce^{-F_{R10}/T} + c^2e^{-F_{T11}/T} + c^2e^{-F_{R11}/T}}{e^{-F_{T00}/T} + e^{-F_{R00}/T} + 2ce^{-F_{T10}/T} + 2ce^{-F_{R10}/T} + c^2e^{-F_{T11}/T} + c^2e^{-F_{R11}/T}} \tag{B30}$$

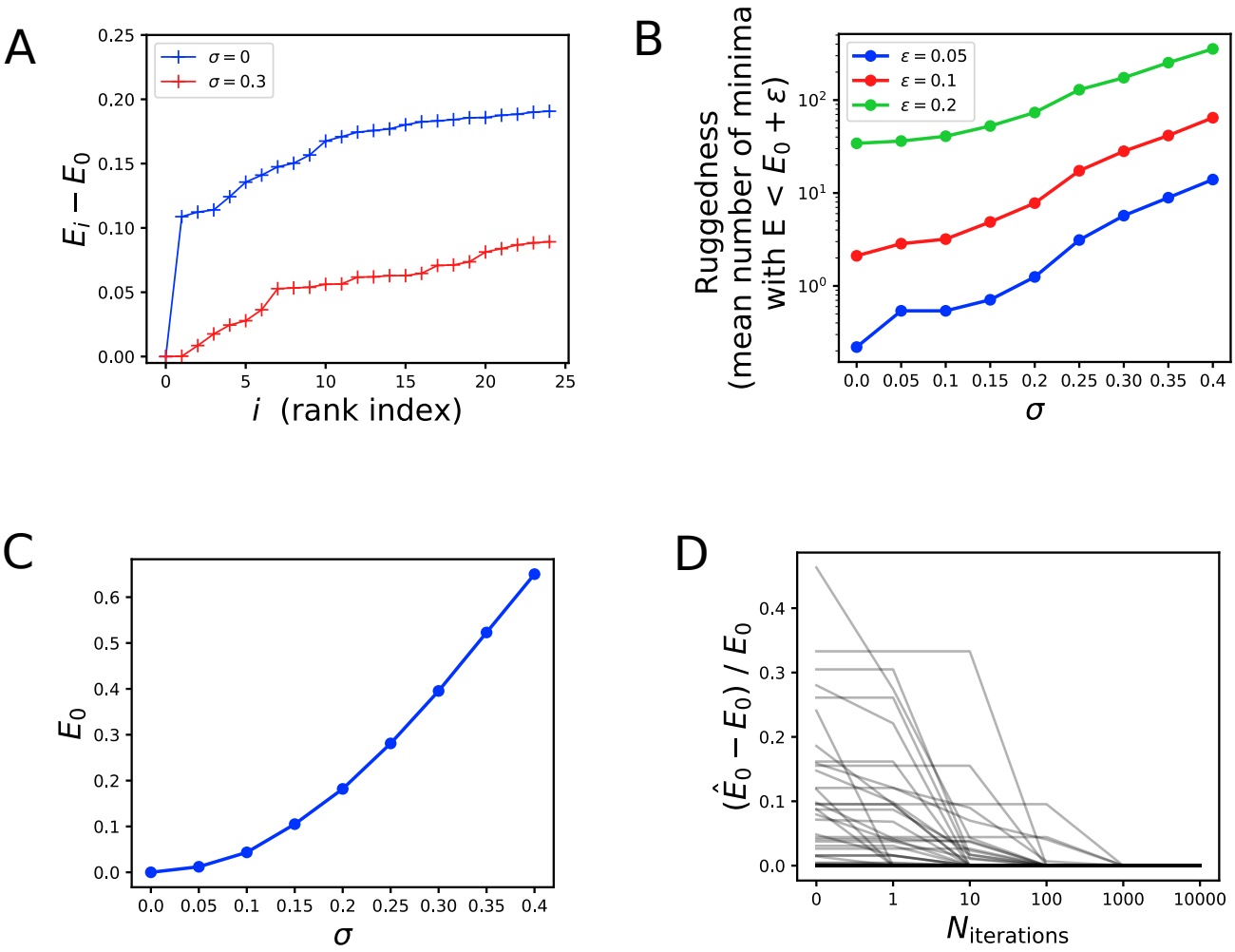

FIG. S1. Ruggedness and frustration increase with σ. (A) The energies of the 25 lowest minima relative to the ground state energy (E_0) for a network with $\sigma = 0$ (blue) and $\sigma = 0.3$ (red). The networks with ordered interactions ($\sigma = 0$) have a ground state far more stable than any other minima, whereas networks with disordered interactions $\sigma = 0.3$ have many near-degenerate low energy states. (B) We measure the ruggedness of an energy landscape as the number of minima within ϵ of the ground state energy (E_0). For each σ, we plot the ruggedness averaged over 100 random networks. Higher σ implies more low energy minima relative to the ground state. Minima are found with the ground-state finding algorithm (Methods). (C) Frustration, the extent to which bonds are stressed, is measured by the ground state energy E_0. A ground state where all springs are relaxed has $E_0 = 0$. For each σ, 100 random networks are generated and their ground states are estimated with the ground-state finding algorithm (Methods). (D) The error in the estimated ground state energy $\hat{E}_0$ for an increasing number of iterations of the ground state finding algorithm for 100 random networks. ($\sigma = 0.3$ and population size $p = 20$). At 100 iterations, 96% of ground state estimates are correct. The energies after 10000 iterations are taken to be the true ground state energies, E_0. These data show that the ground state can be estimated with sufficient accuracy even when the energy landscapes are rugged with many minima.

Appendix C: Supplemental Figures

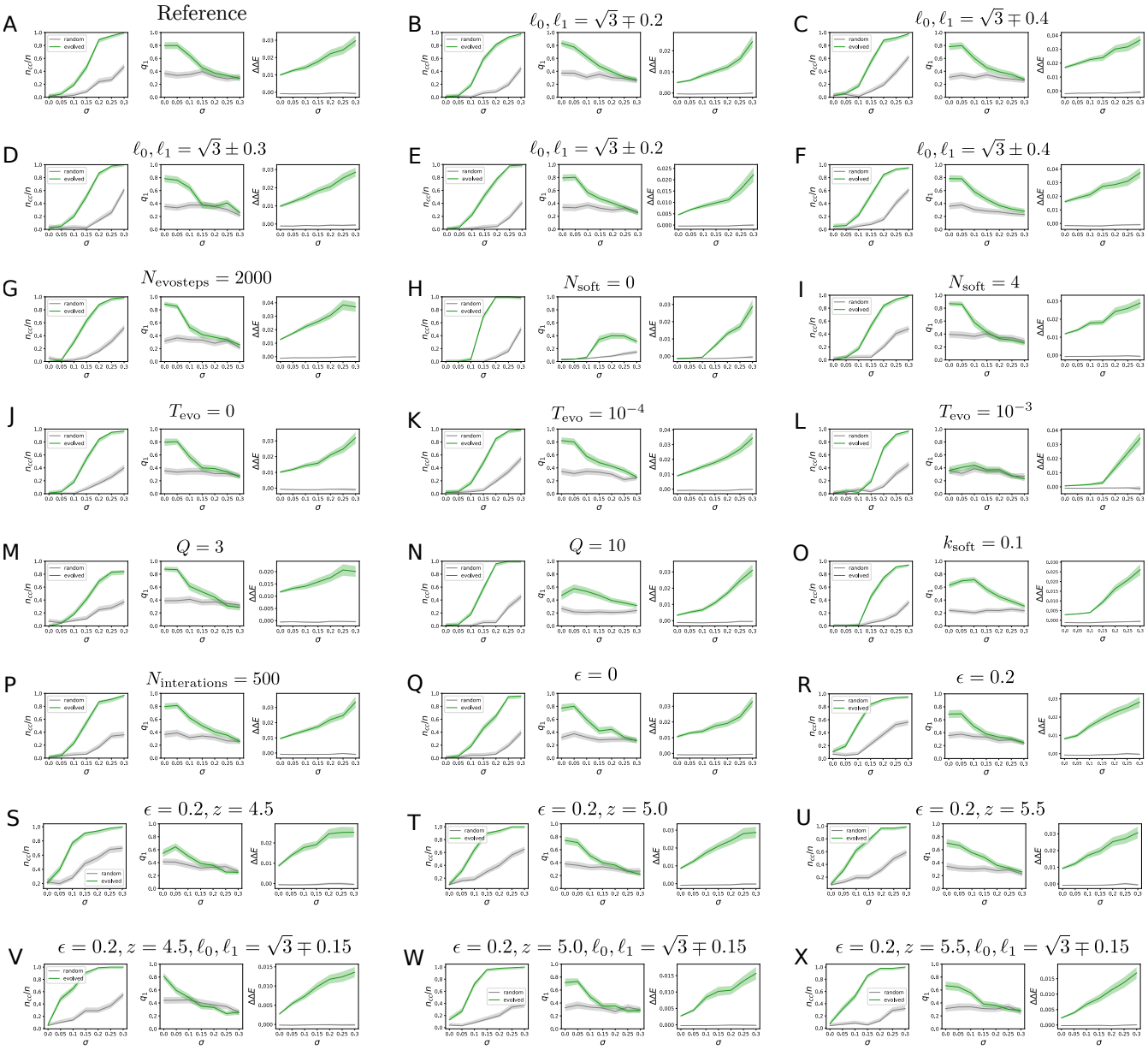

FIG. S2. Robustness of Fig 3AB with respect to various parameters. Each panel shows the fraction of networks that undergo a multi-state conformational change upon binding ligand n_{cc}/n, the mean overlap of the allosteric mode with the softest mode q_1, and the mean cooperativity $\Delta\Delta E$ for 100 random (gray) and evolved (green) networks. In panels B-Q only one parameter is changed from the reference in panel A. (A) Same data as in Figure 3AB where the parameters of the simulation are: $\ell_0 = \sqrt{3} - 0.3$, $\ell_1 = \sqrt{3} + 0.3$, $k_0 = k_1 = 1$, $N_{\text{evosteps}} = 500$, $N_{\text{soft}} = 2$, $T_{\text{evo}} = 10^{-5}$, $Q = 5$, $k_{\text{soft}} = 0.01$, $N_{\text{iterations}} = 100$, and spatial disorder $\epsilon = 0.1$. (B-F) Results do not significantly change with different choices of ligands except that cooperativity decreases when the difference between ℓ_0 and ℓ_1 decreases, as predicted by the 1d model. (G) Results do not change when the number of interactions of the Monte Carlo evolution is increased from $N_{\text{evosteps}} = 500$ to $N_{\text{evosteps}} = 2000$. (H) When there are no soft interactions permitted between nodes, $N_{\text{soft}} = 0$, (i.e. if $K(s_i, s_j) = 1$ for all entries) no cooperativity evolves at low σ. (I) Doubling the number of soft interactions from $N_{\text{soft}} = 2$ to $N_{\text{soft}} = 4$ does not significantly change the results. (JKL) Changing the temperature of the evolutionary Monte Carlo T_{evo} does not change the results as long as it is sufficiently small, $T_{\text{evo}} < 10^{-3}$. At $T_{\text{evo}} \geq 10^{-3}$ nearly no cooperativity evolves at small σ. This result was previously described in[15]. (MN) The results are unchanged with a different number of node types Q. (O) The results are unchanged when the softness of the soft interactions is increased to $k_{\text{soft}} = 0.1$. (P) The results are unchanged if the number of iterations of the basin hopping algorithm is increased from $N_{\text{iterations}} = 100$ to $N_{\text{iterations}} = 500$. (QR) The results are unchanged when the spatial disorder is removed $\epsilon = 0$ (corresponding to $D_{ij} = 0$) or increased $\epsilon = 0.2$. (S-X) The results are unchanged if networks are built with an alternate method where disorder is allowed in the connectivity (A_{ij}). z is the mean coordination (see SI).

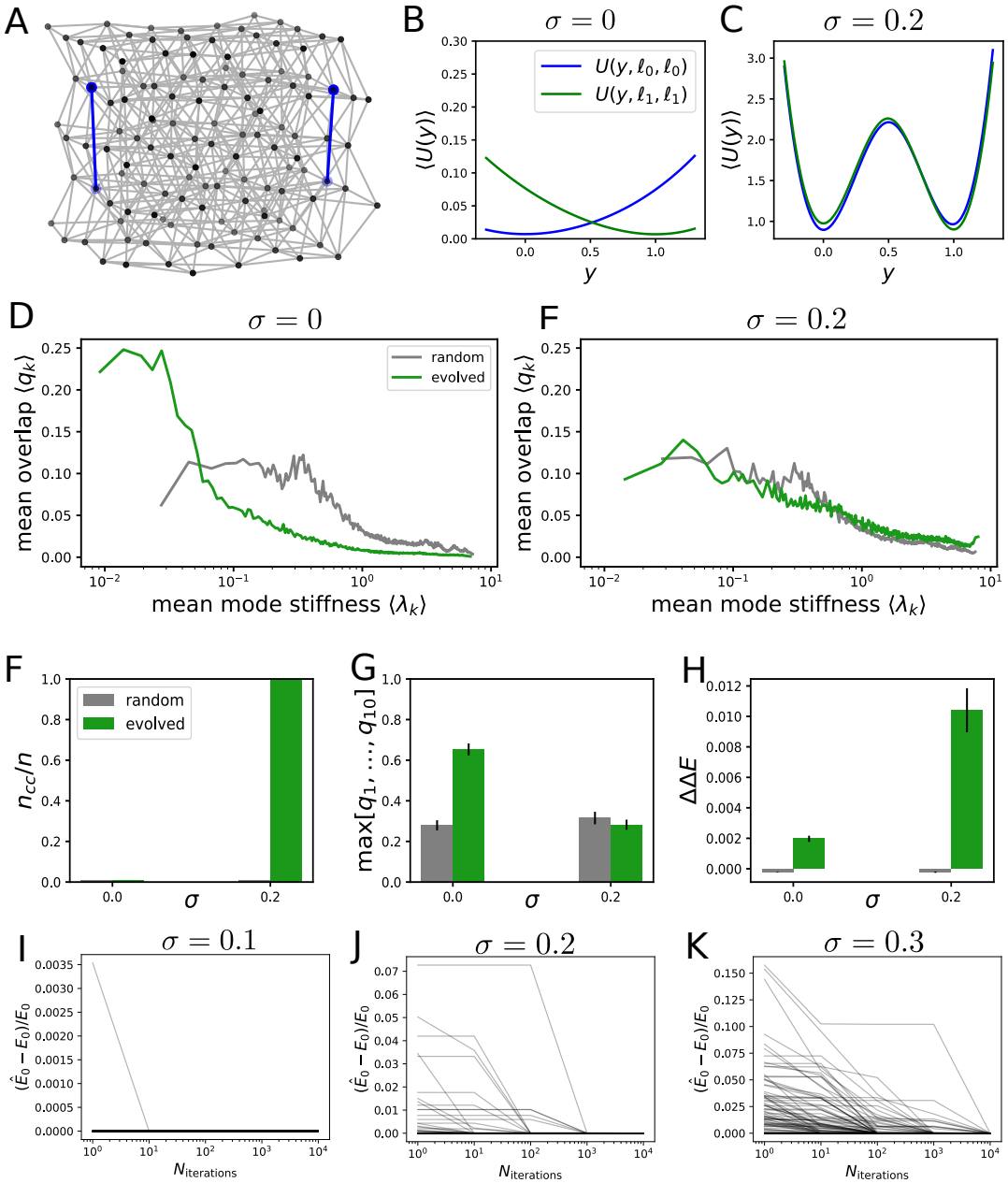

FIG. S3. 3d networks show same behaviors as 2d networks. (a) A visualization of a $5 \times 5 \times 5$ 3d network. Blue springs on opposite sides of the network are the active and allosteric sites. The data in the following subplots are from simulations with the following parameters: $\ell_0, \ell_1 = 2\sqrt{3}/3 \mp 0.15$, $k_0 = k_1 = 1$, $N_{\text{evosteps}} = 10^3$, $N_{\text{soft}} = 2$, $T_{\text{evo}} = 10^{-5}$, $Q = 5$, $k_{\text{soft}} = 0.01$, $N_{\text{iterations}} = 100$, and spatial disorder $\epsilon = 0.1$. (BC) Mean energy of the fully-solvated (blue) and fully-bound (green) networks along the conformational coordinate y interpolating between the two ground state structures $\mathbf{R}_{00}$ and $\mathbf{R}_{11}$ of evolved networks, averaged over 100 replicates. When $\sigma = 0$ (subplot B), the energy has a single minimum, and when $\sigma = 0.2$ (subplot C), energies are bistable. (DE) The mean overlap (averaged over 100 replicates) $\langle q_k \rangle$ between the structural displacement upon binding ligand $\Delta\mathbf{r}$ and each normal mode of the evolved network $\mathbf{v}_k$ ($q_k = |\mathbf{v}_k \cdot \Delta\mathbf{r}/\|\Delta\mathbf{r}\|\ |$) plotted against the mean mode stiffness $\langle \lambda_k \rangle$. When $\sigma = 0$ (subplot D), the softest modes overlap with the allosteric displacement indicative of a single-state mechanism. (F) The fraction of networks that undergo a multi-state conformational change upon binding ligand n_{cc}/n, for 100 random (gray) and evolved (green) networks. (G) The mean of the maximum overlap of the allosteric mode with any of the 10 softest modes q_k, $k = 1, \ldots, 10$, for 100 random (gray) and evolved (green) networks. (H) The mean cooperativity $\Delta\Delta E$ for 100 random (gray) and evolved (green) networks. (IJK) The error in the estimated ground state energy $\hat{E}_0$ for an increasing number of iterations of the ground state finding algorithm for 100 random networks (population size $p = 20$). For $\sigma = 0.2$ and 100 iterations, 95% of ground state estimates are correct. The energies after 10^4 iterations are taken to be the true ground state energies, E_0.

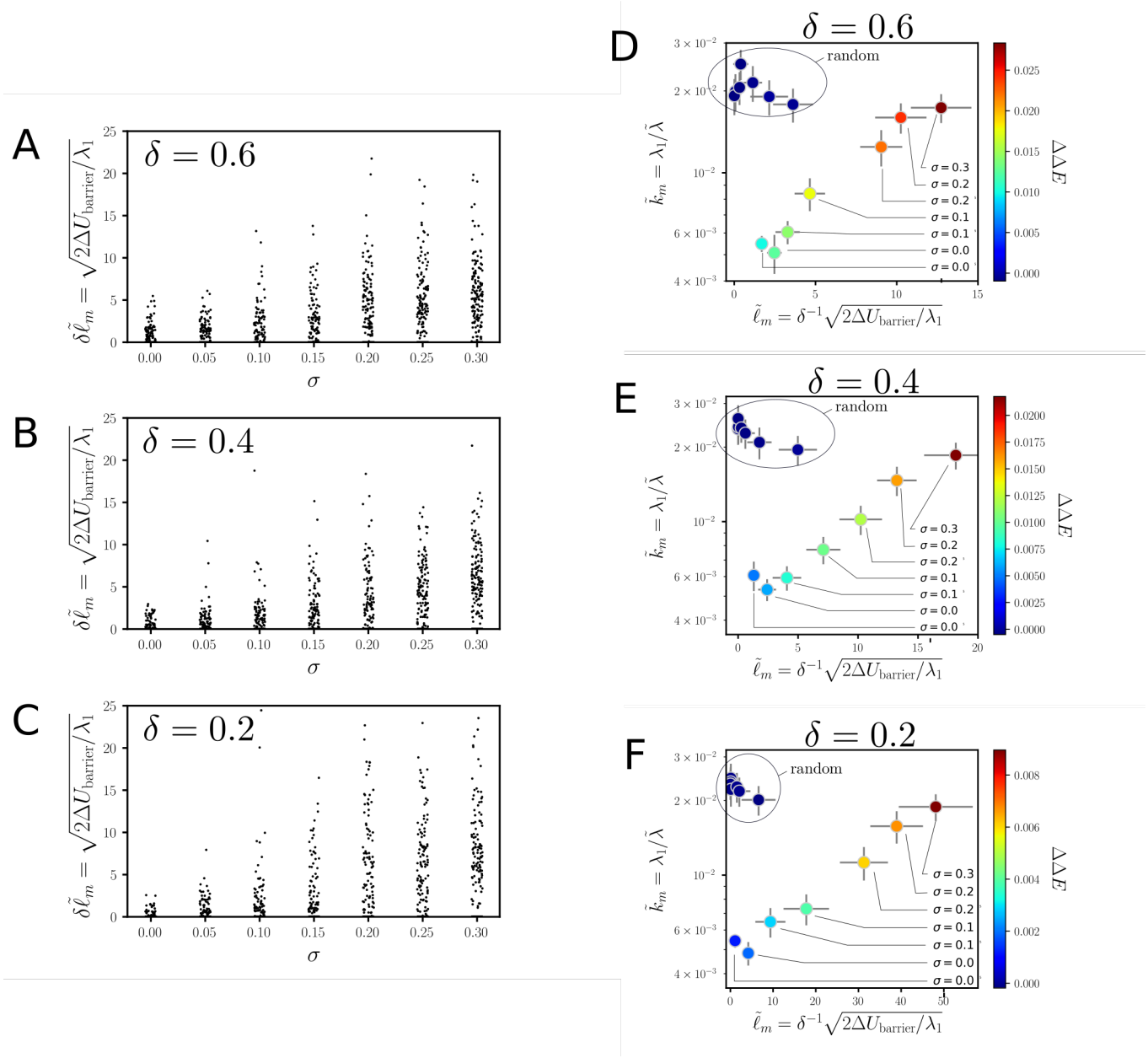

FIG. S4. The properties of the 1d model recapitulate the properties of the 2d elastic network. $\tilde{k}_m$ and $\tilde{\ell}_m$ are the 2d elastic network analogs of the 1d model's reduced parameters k_m/k_a and ℓ_m/δ. See methods for their definitions and motivations. (ABC) For each σ, $\tilde{\ell}_m\delta$ of each of the 100 random and 100 evolved networks is plotted, showing an estimate of the range of possible values of $\tilde{\ell}_m\delta$ given σ. (DEF) The mean $\tilde{k}_m$ and $\tilde{\ell}_m$ and $\Delta\Delta E$ are plotted for 100 random and 100 evolved networks at different σ. Consistent with the 1d model, non-allosteric random networks have a large $\tilde{k}_m$ and small $\tilde{\ell}_m$. When σ is small, networks approach the single-state mechanism limit ($\ell_m = 0, k_m = 0$). As σ increases, networks localize towards the multi-state mechanism limit of large k_m, large ℓ_m. Error bars are 95% CI.

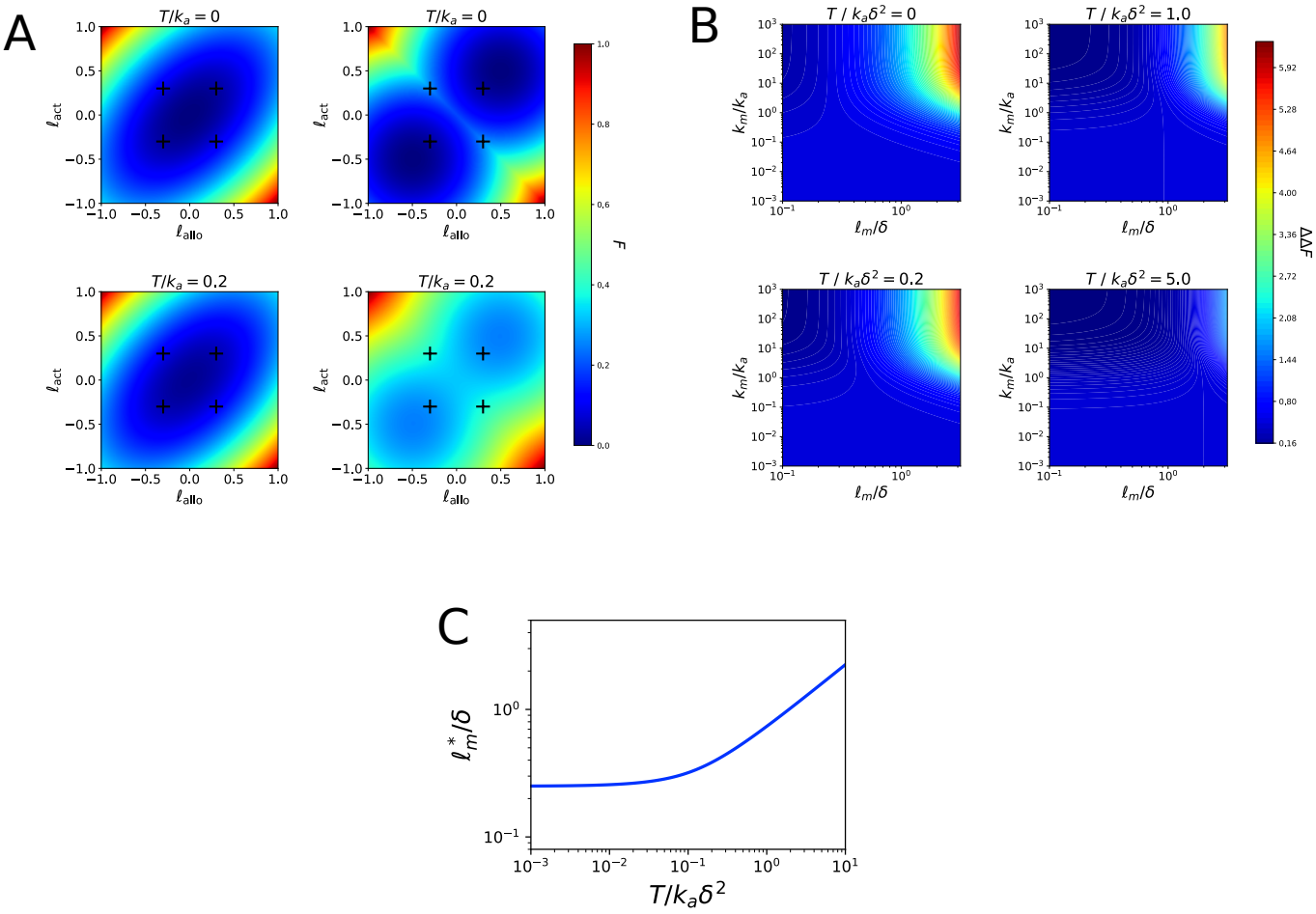

FIG. S5. 1d model at finite temperature. (A) Free energy surfaces as a function of different binding ligands, corresponding to varying the rest lengths $\ell_{\rm act}$ and $\ell_{\rm allo}$ of the springs defining the active and allosteric sites. The two panels on the left show the free energy surfaces of a single-state mechanism ($k_m = 1$ and $\ell_m = 0$) at $T/k_a = 0$ and $T/k_a = 0.2$. The two panels on the right show the free energy surfaces of a multi-state mechanism ($k_m = \infty$ and $\ell_m = 0.5$) at $T/k_a = 0$ and $T/k_a = 0.2$. (B) The cooperativity $\Delta\Delta F$ as a function of the normalized quantities k_m/k_a and ℓ_m/δ for different temperatures. (C) A plot of $\ell_m^*(T)$, the value of ℓ_m where the single and multi-state mechanisms provide equal cooperativity at temperature T.

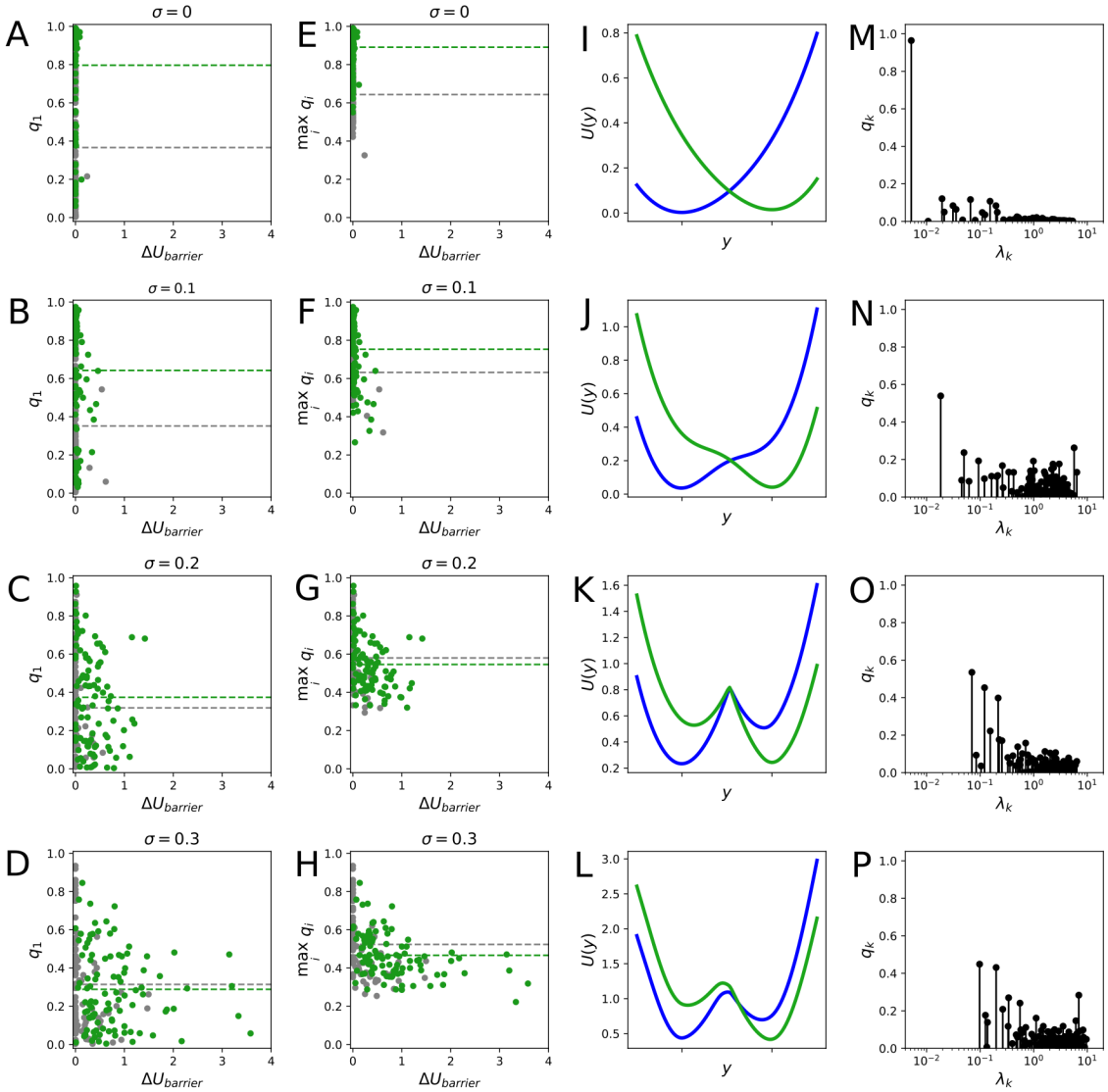

FIG. S6. A continuum of mechanisms exists in the 2d elastic network. (A-D) The barrier height $\Delta U_{\text{barrier}}$ (see SI text for definition) and overlap with the softest mode q_1 is plotted for both random (grey points) and evolved (green points) networks at different values of rest length interaction disorder σ. Grey and green horizontal lines indicate the mean of q_1 for the random and evolved networks, respectively. (E-H) The barrier height $\Delta U_{\text{barrier}}$ and the maximal overlap of the allosteric displacement with any mode, $\max_i\ q_i$ is plotted for both random (grey points) and evolved (green points) networks at different values of rest length interaction disorder σ. Grey and green horizontal lines indicate the mean of $\max_i\ q_i$ for the random and evolved networks, respectively. (I,M) The energy along the allosteric displacement $U(y)$ and the overlaps of each mode q_k vs. the mode stiffness λ_k of an example evolved sequence from the population shown in A and E. (J,N) $U(y)$ and q_k vs. λ_k of an example evolved sequence from the population shown in B and F. (K,O) $U(y)$ and q_k vs. λ_k of an example evolved sequence from the population shown in C and G. (L,P) $U(y)$ and q_k vs. λ_k of an example evolved sequence from the population shown in D and H. The networks in I-P were chosen as examples of when $q_1 \gtrapprox 0.5$ even when energy barriers start to emerge. Networks with multi-state conformational change have $\Delta U_{\text{barrier}} > 0$.